EFFECTS OF RAINFALL VARIABILITY ON SPATIAL ACCUMULATION OF PEAK RUNOFF AND EXCESS RUNOFF DEPTH: LITTLE WASHITA RIVER BASIN, OKLAHOMA, USA

Ali Umaran Komuscu	State Meteorological Service, Research Department, Kalaba, Ankara, Turkey
David R. Legates	Southern Regional Climate Center, Louisiana State University, U.S.A.

This paper demonstrates the spatial variability of surface runoff components, accumulated peak flow (Q_a) and excess runoff depth (R_a), in response to varying distribution of precipitation on a basin scale. A hydrologic representation of the Little Washita Basin, Oklahoma, USA, was developed using HEC-1, a lumped parameter-based single event model. Accumulation of peak flow and excess runoff was computed at 20 locations along the drainage network. The analysis focused on the differences in the spatial and temporal distribution of precipitation while total basin rainfall and basin hydrologic conditions are held constant. The study also relates variability in the surface flow to the storm's duration and depth. The analysis shows that heterogeneous rainfall intensities in both space and time greatly influence peak flow. Uneven spatial distribution of precipitation directly contributes to higher peak flows, particularly in storms of short duration. The larger variabilities with Q_a are observed when rainfall has a nonuniform distribution and high intensities. When the distribution of rainfall was more even, the resulting Q_a and R_a showed less variability. The contribution from new subwatersheds to Q_a in a downstream direction is usually less if the high intensity rainfall areas are located far from the centroid of the basin. Coupled with the steady increase in drainage area in the downstream direction, changes in the magnitude and variability of Q_a decrease. Proximity of high intensity rain cells to basin outlet also gains major importance in the spatial behavior of R_a. The study also shows that for high storm totals, flow volumes and peak flow can be simulated more accurately compared to low storm totals.

INTRODUCTION

Spatial rainfall variability and its impact on runoff has been a subject of much research. A spatially uniform depiction of precipitation to model the rainfall-runoff process is usually applied because of the lack of an adequate resolution of precipitation data and model deficiencies in dealing with variabilities in input data (Beven and Hornberger, 1982). This traditional approach contradicts the fact that rainfall is never uniform nor static (Niemczyowicz, 1988). Precipitation can exhibit considerable variations over both time and space and may vary considerably between storms of similar area and duration (Silverman et al., 1981). Rainfall data traditionally used in hydrologic modeling of watersheds also do not take into account the relevant areal and kinematic properties of intense rainstorms. A single gage, or the average of several gages, is often used to estimate basin precipitation and it is assumed that precipitation is uniformly distributed over the basin, which is usually not true both in space and in time (Gupta and Waymire, 1979). Even where rain gages provide apparently adequate areal coverage, the gages themselves are frequently inadequate in their ability to catch the true rainfall, owing to the effect of the wind, wetting on the walls of the collector, mechanical errors, and other sources (Legates, 1987; Legates and Willmott, 1990). Hromadka (1987a,b) emphasized the importance of the areal distribution of precipitation in rainfall-runoff simulations. He argued that the practice of discretization of the basin into subareas might not be justified without sufficient information on rainfall distribution. Osborn (1984) simulated different rainfall patterns as input for a physically-based model in a portion of the Walnut Gulch (Arizona) Experimental basin. He concluded that the spatial and temporal distribution of precipitation has considerable influence on peak discharges and total runoff. Garbrecht (1991) suggested that timing, intensity, and duration of the rainfall can be assumed uniform over the basin to eliminate any bias due to rainfall distribution pattern. He, however, acknowledges that this assumption puts a limit on basin size.

The extent to which runoff response is affected by spatial variability of precipitation, and how this response changes in the downstream direction, are studied by isolating the effects of nonuniform rainfall behavior from the other runoff modifying factors. More specifically, changes in the accumulated peak runoff (peak flow) and excess runoff depth in the downstream direction are traced by defining the effects of spatial variability of precipitation under real basin conditions. In this study, in contrast to many other studies, hypothetical basin configurations and conceptual precipitation variability settings were avoided to reflect the true nature of a basin's hydrology, and actual storm data were used.

PURPOSE AND SCOPE

This research studies how spatial accumulation of excess runoff depth and peak flow in a small basin vary under changing spatial patterns in storm precipitation where accurate representations of storm cells were obtained by a dense rain gage network. The purpose is to define how the surface flow responds to variability in storm precipitation. The study then demonstrates that precipitation variability can affect surface flow conditions even on small basins. Eight different storms were run through the Hydrologic Engineering Center (HEC-1) model, and flood hydrographs were computed at desired locations. The HEC-1 model is a lumped parameter-based rainfall-runoff model. It allows the simulation of a complex rainfall event on hydrologically complex basins and simulates single storms characterized by highly variable precipitation on various spatial scales. The time distribution of runoff during and shortly after a storm event can be also accurately simulated with the time steps of the HEC-1 model.

The study area selected for this research is the Little Washita River Basin, which is a tributary of the Washita River in southwest Oklahoma (Figure 1). The basin is in the southern part of the Great Plains of the United States. It has been under extensive soil and water conservation treatments nearly for the past fifty years. In 1936, a national demonstration project for soil erosion control was initiated in the eastern portion of the basin. Since the 1940s, the U.S. Department of Agriculture's (USDA) Soil Conservation Service (SCS) has applied extensive soil and water conservation structures and measures in the watershed (Staff, 1991). In 1961, The USDA's Agricultural Research Service (ARS) began collecting hydrologic data in the watershed to determine the downstream hydrologic impacts of the flood structures. The data collection process included installation of an extensive rain gage network and a stream gauging station in the watershed. In 1978 the Little Washita River Watershed was chosen for the Model Implementation Project (MIP) to demonstrate the effects of intensive land conservation treatments on water quality in the watershed. The project was jointly sponsored and administered by the USDA and U.S. Environmental Protection Agency (EPA). It should be noted that the purpose of this study is not to investigate runoff characteristics peculiar to the Little Washita River Basin. The basin was selected because of the availability of hydrologic and meteorological data at the desired resolution and quality. It is our hope that the results of the study might be of great use for the Little Washita Basin and other basins with similar nature and where intensive land treatments are applied. Although the focus of this study is not to address water supply or pollution issues directly, an improved understanding of spatial distribution of runoff would be beneficial to assessment of water resources availability and non-point source pollution potential for other locations with similar climatic and hydrologic conditions.
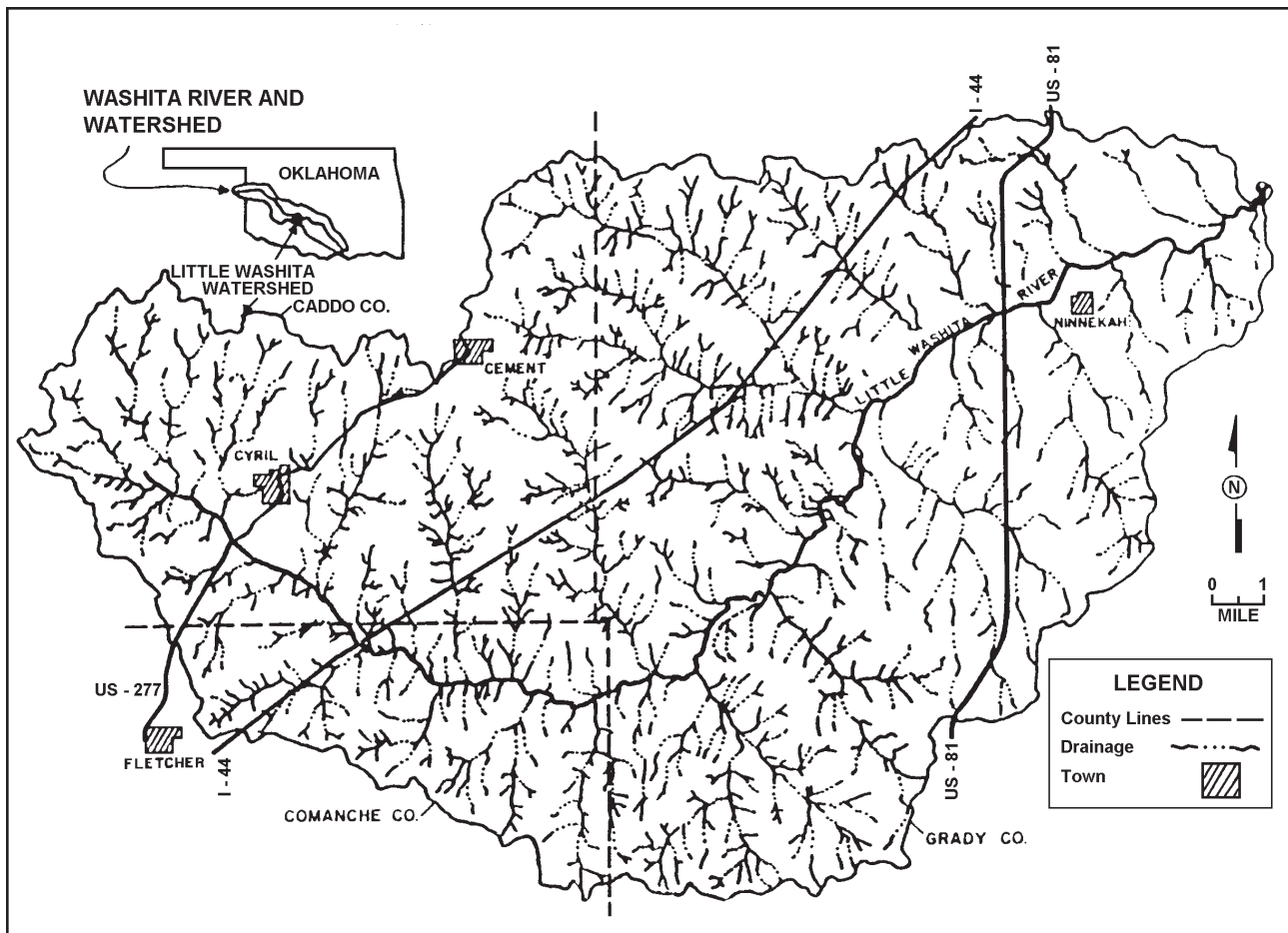

Figure 1. Location and map of the basin.

The basin area is 539 km^2 and extends across portions of Grady, Caddo, and Comanche counties. The general physical characteristics of the basin are described in detail in ARS (1983) and Allen and Naney (1991). Soil surveys indicate that the hydrologic soil group B is the most dominant soil type in the basin area, covering nearly one third of the basin (Allen and Naney, 1991). Soil group D, on the other hand, makes up the smallest coverage with 1.6 percent. Soil surveys define different soil series and 162 soil phases reflecting different surface soil textures, slopes, degree of erosion, and other characteristics within a soil series. These surveys have been updated and a new classification system has been developed which defines 103 different soil clusters (Salisbury, 1992). An unsupervised classification of the 1974 Landsat image indicated that approximately 64 percent of the basin was covered by pasture in varying conditions while crops and woodland made up 21 percent and 13 percent of the basin, respectively (Komuscu, 1993). The Little Washita River Basin has a dense rain gage network with 36 recording rain gages. There are also two stream gages located in the basin (Figure 2a).
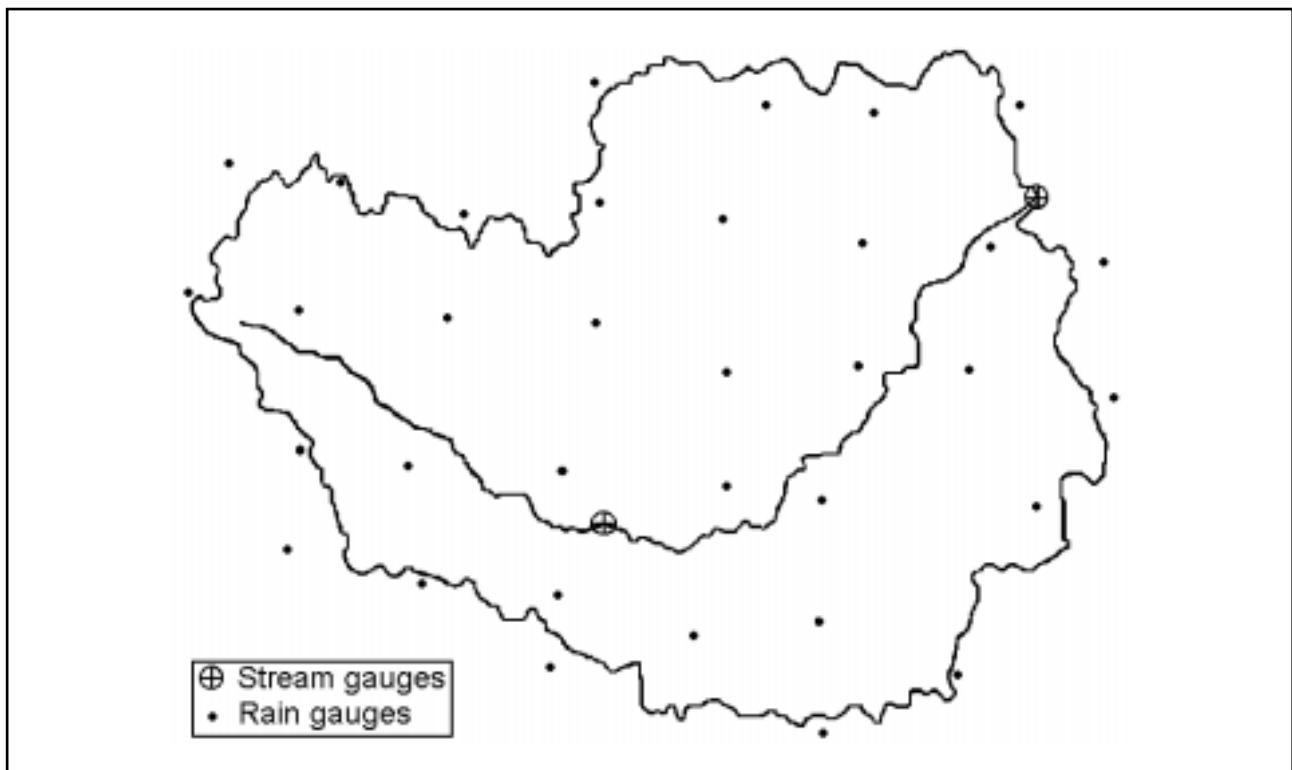

Figure 2a. Location of the rain gages and stream gages in the basin.

MODEL DEVELOPMENT

Preparation of the basin for simulation

A complete scheme of the HEC-1 model development, which includes three separate phases, is shown in Figure 3. The sub-basins are characterized by the topography and stream channel network. Nicks (1985, 1986) used a subdivision system based on geologic and vegetation characteristics of the basin to simulate basin-scale runoff and sediment yield. Duchon et al. (1990, 1992) derived a subdivision scheme based on the vegetation types and simulated the water budget of the Little Washita River Basin. Basin boundaries were delineated using the 1:24000 USGS topographic maps for the Apache, Cyril, Laverty, East Ninnekah, Rocky Ford, Fletcher, and Rush Springs quadrangles. Stream ordering was accomplished by digitizing the channels from topographic maps. After the drainage network was obtained, sub-basins were delineated based on the slope, relief, and channel
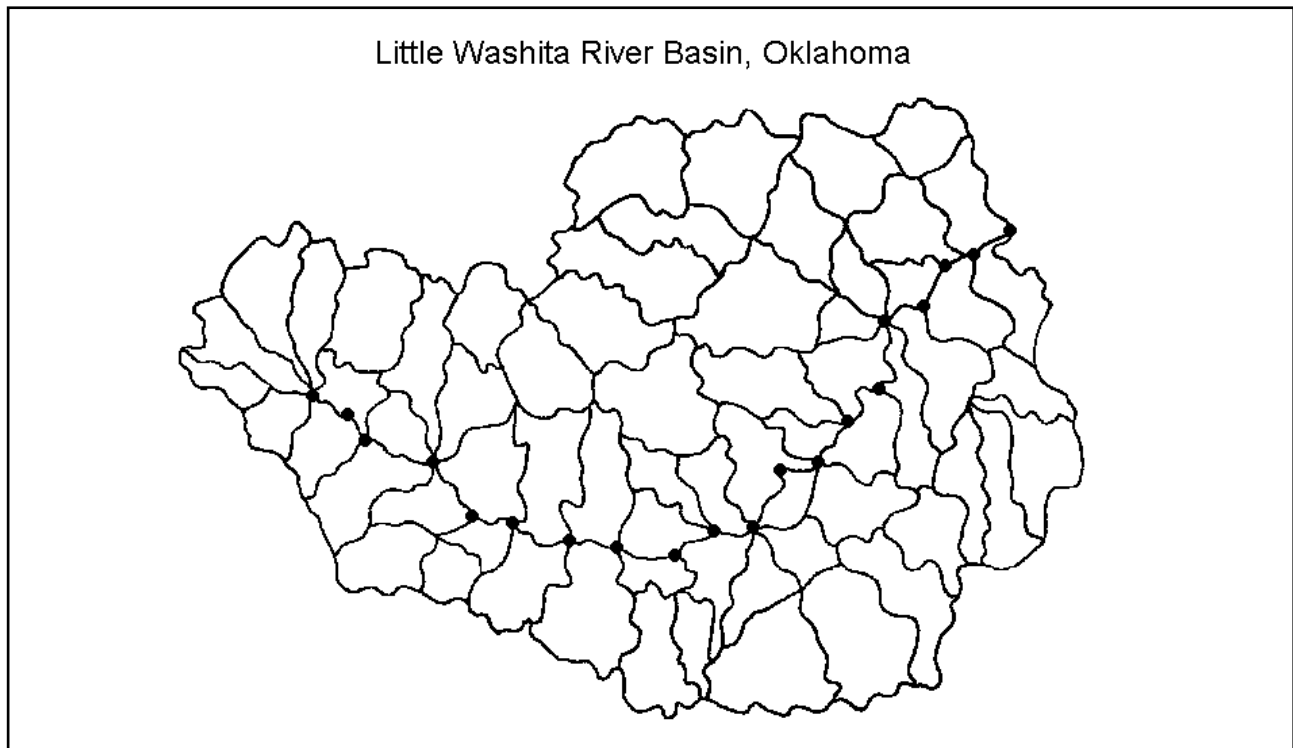
Figure 2b. Subdivision and runoff computation points used for the simulation.
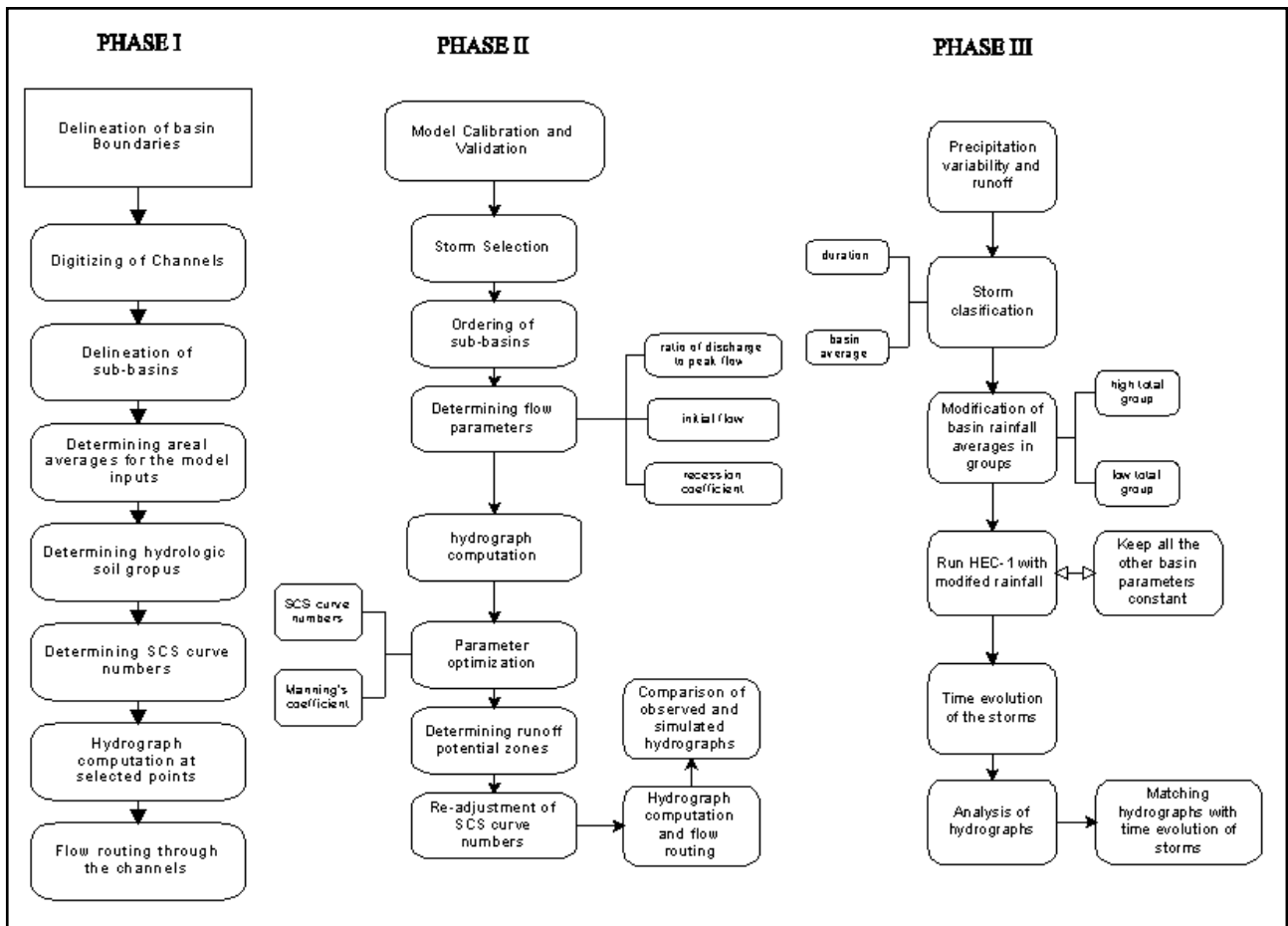

Figure 3. HEC-1 model development for hydrograph simulation in the Little Washita River Basin.

configuration of the basin. A total of 66 sub-basins varying in size from 3 km^2 to 15.6 km^2 was delineated (Figure 2b). The sub-basins were intended to be as small as possible since the assumption of uniform precipitation becomes more accurate with smaller sub-basins. Komuscu (1993) gives complete details of the parameterization of the basin using the HEC-1 model.

Incremental storm precipitation data recorded at the thirty-four gages located in and around the basin were used in the study. Precipitation rates for the gages, which had only storm totals, have been obtained using the information from nearby gages with similar temporal and spatial storm patterns (storm direction, storm speed, and position of the advancing storm front). Basin average precipitation amounts and temporal precipitation patterns were calculated using the Thiessen polygon method. Criteria for selecting individual rainfall-runoff events included conditions where snowfall and snowmelt were insignificant, rainfall durations were at least one hour or more, and a basin average precipitation of at least 3.0 mm were observed. Storm events were selected from different ranges varying from 3.3 to 52.3 mm in basin average rainfall. It should be noted that the word 'storm' is not meant in the strict meteorological sense; rather it refers to the synoptic situation of storm weather conditions. Another observed hydrometeorological variable used in this research is streamflow discharge for the selected storms. The observed streamflow discharge is not a model input but is used to calibrate other model parameters. The precipitation and streamflow records for the selected storms were provided by the United States Department of Agriculture's National Agricultural Water Quality Laboratory in Durant, Oklahoma.

The model requires an assessment of soil types, topography, and land-use conditions for the basin. First, hydrologic soil groups were determined for each sub-basin on the basis of runoff potential, infiltration capability, soil types, soil structure and depth of the soil layers. Next, curve numbers were computed based on the hydrologic soil groups, land-use types, and antecedent moisture conditions. The original values of the curve numbers for the corresponding land-use types in the Little Washita River Basin were taken from Salisbury (1992). The land-use and soil types in each sub-basin were obtained from the 1974 Landsat images. The spatial distribution of soil and land-use types was cross-tabulated to determine the proportion of land-use for the individual soil groups.

Accumulated peak flow rate and excess runoff depth were computed for each subbasin and routed to hydrograph combination points selected along the drainage network. Changes in the accumulated peak runoff rates and excess runoff depths are traced as the runoff moves downstream. Along the drainage network, the accumulated peak flow rate and accumulated excess runoff depth are referred to as Q_a and R_a, respectively. The study uses the curve number method developed by the Soil Conservation Service (SCS) for obtaining excess runoff depth. The SCS dimensionless unit hydrograph method was used to convert the rainfall excess to runoff hydrograph, and the peak flow rate for individual subbasins was estimated. The ordinates of the unit hydrograph are determined through interpolation of the dimensionless unit hydrograph curve at points defined according to a specified computational interval (Hoggan, 1989). Complete details of the SCS curve number and SCS dimensionless unit hydrograph methods are described in Section 4: Hydrology, National Engineering Handbook, Soil Conservation Service (1964). The 'standard' finite difference form of the kinematic wave approximation of the Saint-Venant equation is used for flow routing through the channel network. Data required by the kinematic wave method were obtained from the channel cross-section surveys done by the USDA Water Quality Lab, Durant, Oklahoma. The channel cross sections were used to extract the required information on channel bottom width, channel shape, and side slopes. Channel roughness is represented by the Manning's channel roughness coefficients.

Model Calibration and Validation

After subdividing the basin into small topographic units, the model is calibrated and validated using observed rainfall events. As the interior streams lacked streamflow data for the simulation period, only the gage at the basin outlet is used for the calibration and validation. Calibration of the model is accomplished by trial and error in which a hydrograph is computed for an initial set of parameters and compared with the observed hydrograph. The parameters are then adjusted on the basis of the comparison until a satisfactory fit is obtained. The storm event of May 9, 1964, which produced a basin average rainfall of 52 mm of rainfall over a 3.7 hour period, was used to calibrate the model. The highest point precipitation measured for this storm was 102.3 mm at gage 163. Fifteen minute precipitation intensities ranged from 0.25 to 72.1 mm per hour. The first step in the calibration was to order the sub-basins for runoff computations and streamflow routing from upstream to downstream. When routing is performed, the hydrograph from an upstream basin is treated as the inflow hydrograph for the immediate downstream basin. The second step in the calibration was to determine the initial flow from antecedent runoff, the ratio of discharge at which recession flow begins to the peak flow, and the recession coefficient. These three base flow parameters were obtained from the logarithm of observed streamflow discharge versus time for the calibration period. The peak flow resulting from this event was 218 m^3s^{-1}, which occurred approximately 7.75 hours after the event began. Curve numbers were categorized as SCS Type II based on antecedent conditions prior to the onset of the storm. The computational interval used in the calibration was 15 minutes, reflecting time intervals of both the measured hyetograph and the measured hydrograph. The simulation length was 22.25 hours-from 1930 CST on May 9 to 1745 CST on May 10, 1964.

Calibration was then accomplished by adjusting the SCS curve numbers and Manning's channel roughness coefficient. First, the original measured or estimated values for the model parameters were used to simulate streamflow. Initial results indicated that the SCS curve numbers were relatively low which resulted in an underestimation of peak flow and total flow volume. Underestimation of these components on the hydrograph was not surprising since the model parameters did not take into account the antecedent moisture conditions. As a small storm occurred prior to the calibration storm, the ground was fairly wet. Wetter moisture conditions, however, were not reflected in the original curve numbers. To compensate for the differences between observed flow and the model simulated flow, the curve numbers were adjusted. First, the watershed was divided into different runoff potential zones based on soil permeability, soil depth, and soil types. The procedure resulted in four different runoff potential areas ranging from high runoff potential to very low-runoff potential. Next, the curve numbers in these sub-basins were increased slightly until a reasonable similarity between the observed and simulated hydrographs was reached. The next step was to improve the time of peak flow by adjusting the Manning's channel roughness coefficient for the selected routing channels. The adjustment of Manning's roughness coefficient is necessary to produce a realistic outflow hydrograph since the kinematic wave routing provides a solution to the physical equations only for one-dimensional flow, whereas the actual watershed flow is two-dimensional (Chow et al., 1988). Thus, Manning's roughness coefficients were set at 0.048 for the upstream areas to reflect the rough to smooth flow conditions. As the flow is routed downstream, the coefficient was reduced slightly to represent the smoother flow conditions due to an increase in velocity and volume of the flow. The HEC-1 model uses a numerical index of closeness of fit of observed and simulated streamflow over the entire storm event. This objective function is the square root of the weighted square (RMS) difference between the observed hydrograph and the computed hydrograph. It provides a degree to which the simulated hydrograph matches the observed hydrograph on a variety of factors, including

peak discharge, time of peak discharge, and total runoff volume. The difference between the simulated and observed hydrographs will be a minimum for the optimal parameter estimates. The objective function (ST_f) is computed from

$$ST_f = \left[\sum_{i=l}^{n} (Q_{obs} - Q_{com})^2 W_t / n \right]$$

(1)

where

Q_{com} is the ordinate of the runoff hydrograph for time period i computed by HEC-1, Q_{obs} is the ordinate of the observed runoff hydrograph, n is the total number of hydrograph ordinates, and W_t is the weight for the hydrograph ordinate i computed from

$$W_t = \frac{(Q_{obs} + \overline{Q})}{(2\overline{Q})}$$

(2)

where

Q is the average observed discharge (U.S Army Corps of Engineers, 1990). The equation gives more weight to the accurate simulation of peak flows rather than low flows by biasing the objective function.

Final calibration results illustrate that the flow volume, peak flow, equivalent depth of flow, and mean flow are simulated reasonably well although the time to peak is still not reproduced accurately (Table 1). Further calibration attempts indicated that improving this component would diminish the accuracy in other components of the simulated hydrograph. The calibration is considered adequate because the computed hydrograph simulates the rising and falling limbs, flow volume, mean flow, and equivalent depth fairly well. Expectations of a better simulation are perhaps unrealistic because it is difficult to incorporate the manner in which antecedent moisture conditions modify the initial

Table 1. Characteristics of the Storms Selected for the Rainfall-Runoff Simulaton

Date	Point Max (mm)	Duration (hr)	Max. Rate (mm/hr)	Basin Ave. (mm)
May 9, 1965	102.3	3.1	72.1	52.3
May 10, 1964	47.5	14.3	30.4	21.6
August 18, 1964	50.3	3.3	29.7	37.3
November 16, 1964	52.3	10.4	19.6	35.6
May 9, 1965	62.7	2.9	22.4	15.0
May 10, 1965	11.0	1.4	3.0	7.4
September 19, 1965	47.8	13.2	16.8	31.2
September 20, 1965	21.1	15.1	17.5	3.3

abstractions. Some simulation errors can also be attributed to simplifications of the HEC-1 model (Cline, 1988).

Validation of the model's capability to simulate the observed flow was accomplished using a storm event that occurred on May 9, 1996 - exactly one year later. This particular storm was selected because it was similar to the calibration storm event with respect to antecedent moisture conditions since a small storm also had occurred immediately prior. Another reason this storm was selected was to test the ability of the model to simulate runoff with a smaller magnitude storm as opposed to the larger magnitude storm used for initial calibration. For the validation, the same SCS curve numbers and the basin lag-times used in the calibration were applied for each sub-basin without any modification while the Manning's channel roughness coefficients were slightly modified to represent rougher flow conditions. The statistical comparison of the observed and computed flows also indicates that the observed flows were simulated more accurately when compared to the calibration simulation (Table 2). Both the objective function and average absolute error are relatively small, reflecting a reasonable model validation. Complete details of the calibration and validation of the HEC-1 model are given by Komuscu (1993).

Table 2. Classification of the Selected Storms for the Raifall-Runoff Simulation After Modifying the Basin Totals

Category I	Basin Rainfall	Duration	Simulated Rainfall (mm)
May 9, 1964	high	short	38.1
August 18, 1964	high	short	38.1
November 16, 1964	high	long	38.1
September 19, 1965	high	long	38.1
Category II			
May 9, 1965	low	short	13.7
May 10, 1965	low	short	13.7
May 10, 1964	low	long	13.7
September 20, 1965	low	long	13.7

ANALYSIS AND RESULTS

After calibrating and validating the model using observed streamflows, the impact of spatial variations of precipitation on spatial accumulation of peak flow and excess runoff depth were investigated. For this purpose, eight storm events which occurred during 1964 and 1965 were selected (Table 2). These storms lasted from 1.4 to 15.1 hours in duration, had maximum observed rainfall rates from 30 to 72.1 mm per hour, and produced basin average rainfalls between 3.30 and 52.3 mm. In all but one storm, the maximum observed rainfall rate exceeded 15 mm per hour during a fifteen minute time interval.

Isolating the impact of precipitation variability on the simulation of the subwatershed peak flow and excess runoff depth was done in two steps. First, the eight storms were divided into groups based on duration and the basin average rainfall. This categorization resulted in two groups, each having four storms similar in basin average rainfall but varying in duration. Storms with identical basin average rainfall and with similar durations were then matched. This resulted in two pairs of storms

Table 3. Summary Statistics for Calibration of the Model Using the May 9, 1964 Storm

	Volume (m³)	Mean Flow (m³/s)	PeakFlow (m³/s)	Time of Peak (CST)
Observed Flow	5310	35.4	213.6	
Computed Flow	5400	35.9	203.0	7.45
Difference	90	0.5	10.6	6.45
Percent change	-1.7	-1.4	-4.9	-1.00
Standard Error	16.8 m³s⁻¹			
Objective function	11.9 m³s⁻¹			
Average absolute error	24.9 m³s⁻¹			
Average percent absolute error	55.0			

in each category with varying duration but similar basin average rainfall (Table 3). Next, the gage-measured rainfall for each storm in the high rainfall total group was modified so that a basin average rainfall of 38.1 mm (1.5 in.) was produced. Similarly, the gage-measured rainfall for each storm in the low rainfall total group was modified so that a basin average rainfall of 12.7 mm (0.5 in.) was produced. If S is the standard depth of precipitation, R is the observed mean basin precipitation obtained by the Thiessen polygon method, and R_{ij} is the measured precipitation at gage j for time i, then

$$R_{ij} = R_{ij} \frac{S}{R} \qquad (3)$$

where

R_{ij} is the standardized precipitation at gage j for time I (Legates and Komuscu, 1997). These modifications were made so that the storms in each group would have produced the same basin average rainfall but varied in the temporal and spatial distribution. The objective was to assess the impact on the resulting runoff hydrographs by varying the temporal and spatial distributions of precipitation while the basin average rainfall remained the same.

The second step in isolating the impacts of the temporal and spatial scales in simulating the runoff was to keep the basin conditions and land use constant throughout the simulations. This was achieved by keeping all model parameters, including lag-times, curve numbers, initial abstractions, base flow parameters, and channel routing parameters constant. Thus, this analysis will focus on the differences in the spatial and temporal distribution of precipitation while total basin rainfall and basin hydrologic conditions are held constant, not the simulation of a real storm event. Dates will be used to delineate one storm pattern from another but they do not refer to the real storm event.

Inferences about the behavior of the simulated storm runoff hydrographs are based on the spatial and temporal organization of the storms. The time evolution of the storm was examined through successive fifteen minute isohyets. Information about the development, movement, and decay, through both time and space, is used to explain the response of the Q_a and R_a to different

representations of the spatial and temporal distribution of precipitation. Due to large number of isohyetal maps, illustration of the time evolution of the storms was limited to early hours of the storms.

Category I Storms

The first evaluation focuses on the May 9, 1964 and the August 18, 1964 storms which are characterized by high rainfall totals and short durations. The May 9, 1964 storm originally develops in the southwestern part of the basin, and moves rapidly to the northeast with increasing intensity. Within the first 30 minutes of the storm, three major high intensity rain cells develop, covering a large portion of the basin (Figure 4). These cells continuously feed streamflow with rapid runoff, causing a steady increase with the peak flow (Figure 5). By the end of the first hour, the storm almost covers the entire basin. The main reason for the low peak flow observed with this storm is the fact that the greater portion of the rain fell in the first 45 minutes of the storm. In other words, the contribution from the addition of the new subwatershed to the peak flow remained very low, and no significant runoff occurred. It has been argued that fast moving storm cells tend to produce lower peak runoff rates (Stephenson and Meadows, 1986). Similarly, the accumulated runoff depth (R_a) experienced a considerable increase in response to the high intensity cells (Figure 5). However, as the storm moved rapidly eastward, the nonuniform feature of the storm disappeared, and additions of the new subwatersheds did not change the magnitude of R_a significantly. For the August 18, 1964 storm, several high rainfall intensity cells develop during the first hour of the storm, which are mainly concentrated around the southwestern part of the basin (Figure 6). However, most of these rainfall maximums occurred far from the basin outlet. Moreover, high-intensity cells within this storm did not last long, and they were mainly replaced with lower intensity cells throughout the storm's duration. This explains why R_a in the downstream direction varies insignificantly. As the number of subwatersheds and the upstream drainage area increases, variability of R_a decreases toward an average value, which is a more representative of the entire upstream drainage area.

The second simulation included the September 19, 1965 and November 16, 1964 storms which are characterized by high rainfall totals and longer durations. The most noticeable features of the accumulated peak flows for these storms are a sudden rise in the upstream area, a leveling off in the centroid of the basin, and another rise close to the basin outlet (Figure 5). A major difference in the accumulated peak flow rates of the two storms, however, is observed with location of the peaks. In the case of the November 16, 1964 storm, runoff contributions from the central subwatersheds to the accumulated peak flow are relatively less. The precipitation distribution with the November 16, 1964 storm exhibited the presence of high rainfall intensity areas close the outlet (Figure 7). Another noticeable feature of this storm is its temporal distribution. Most of the rain within the storm falls in the early hours, which can easily trigger a peak near the outlet (Figure 5). Moreover, despite the intensity of the storm decreasing gradually toward the end of the storm's duration, the individual storm cells still cover the greater portion of the basin. On the other hand, high rainfall intensities in the September 19, 1965 storm were located relatively far from the outlet (Figure 8). Similarly, individual storm cells emerged in the upstream and central parts of the basin, which can result in an increase in Q_a in downstream direction. The accumulated runoff depths for the both storms display similar trends; a high runoff depth upstream and a gradually decreasing trend downstream (Figure 5). There is little variability in the excess runoff volumes of the both storms. A slight rise in R_a toward the basin outlet with the November 16, 1964 storm is possibly due to continuously developing runoff-producing rain cells near the outlet. The rainfall excess from these slow moving cells is probably the main cause for the initial increase in the accumulated peak flow observed with the November 16, 1964 storm.
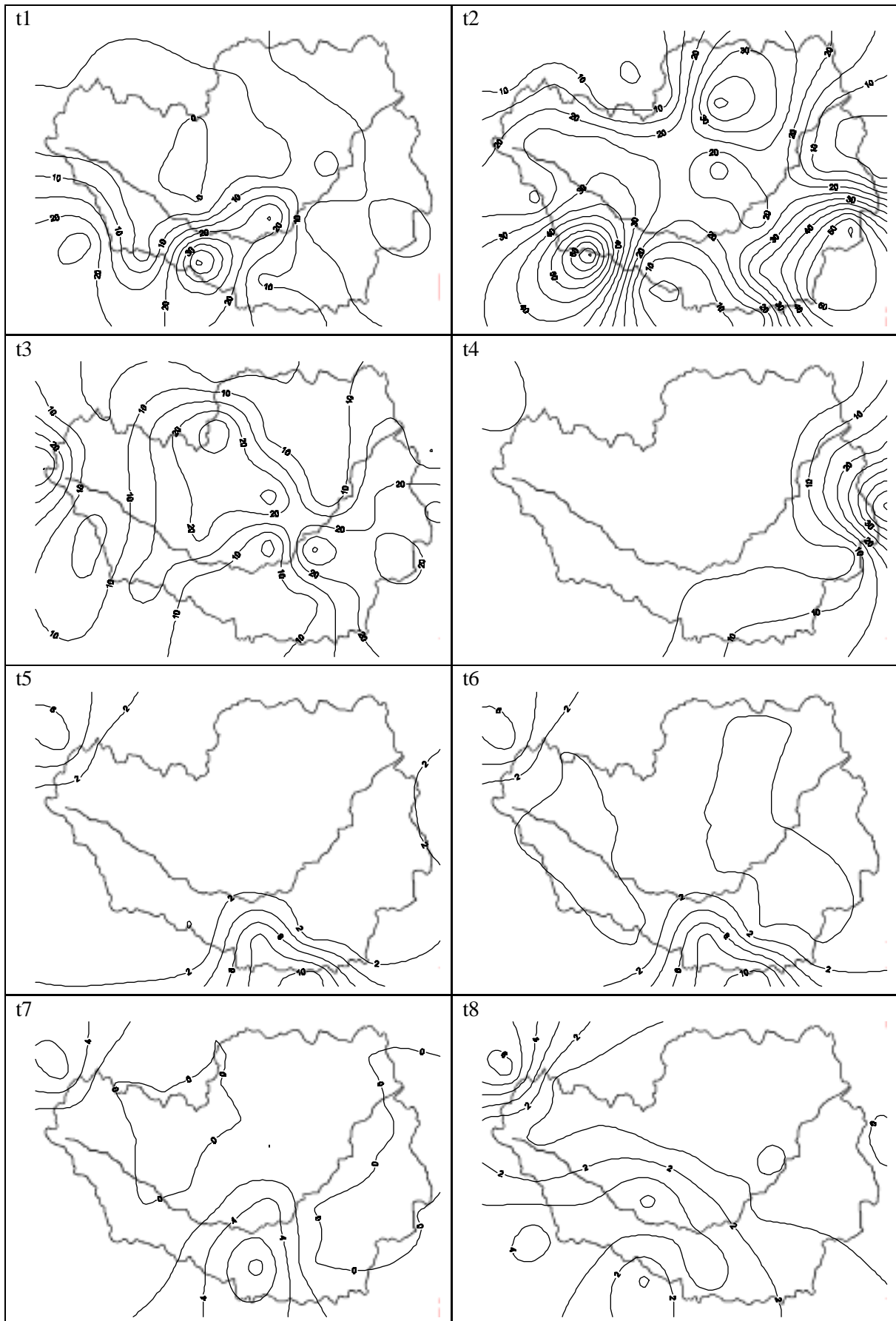
Figure 4. May 9, 1964 storm 15-minute consecutive rainfall distribution pattern.
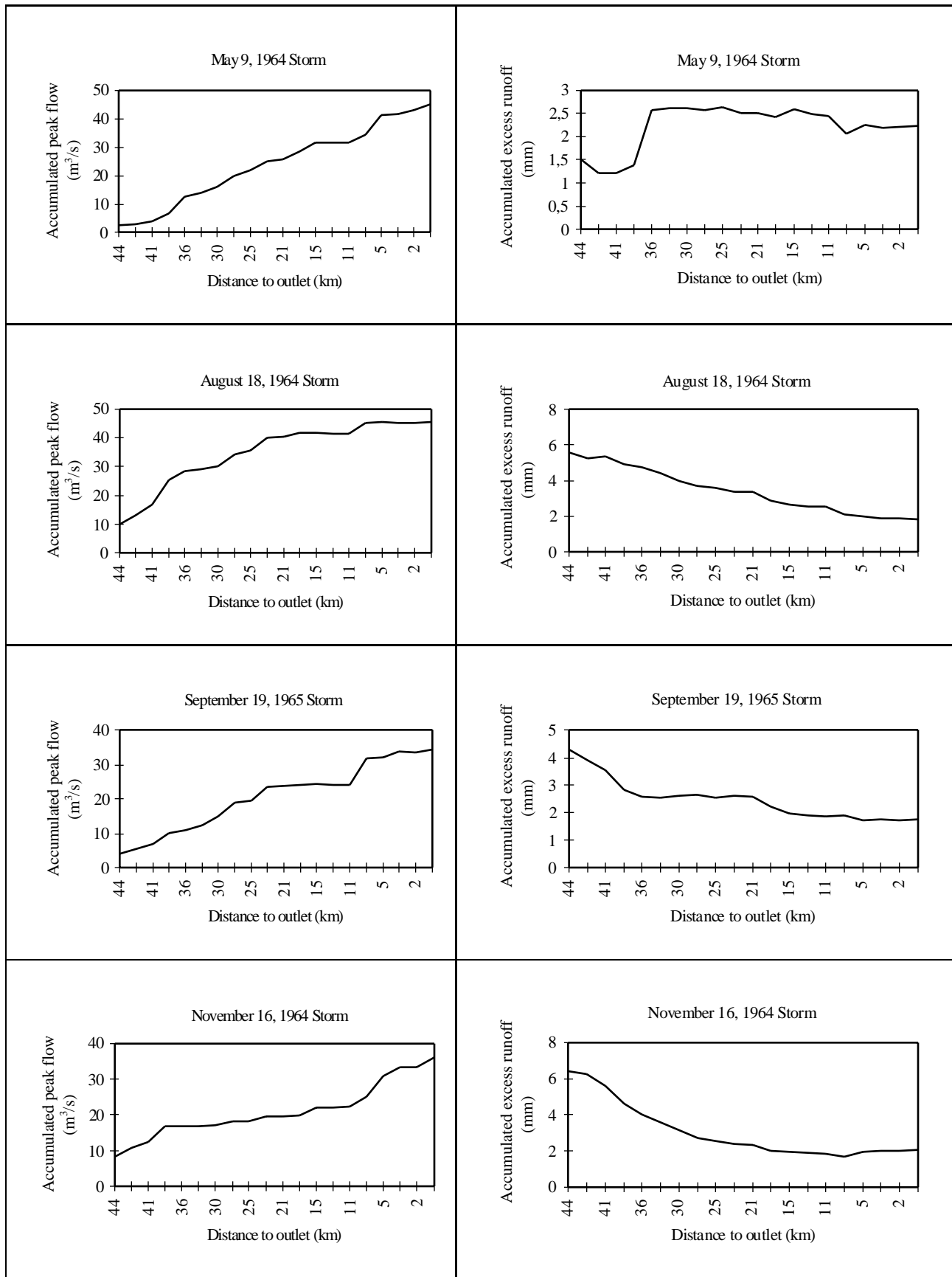
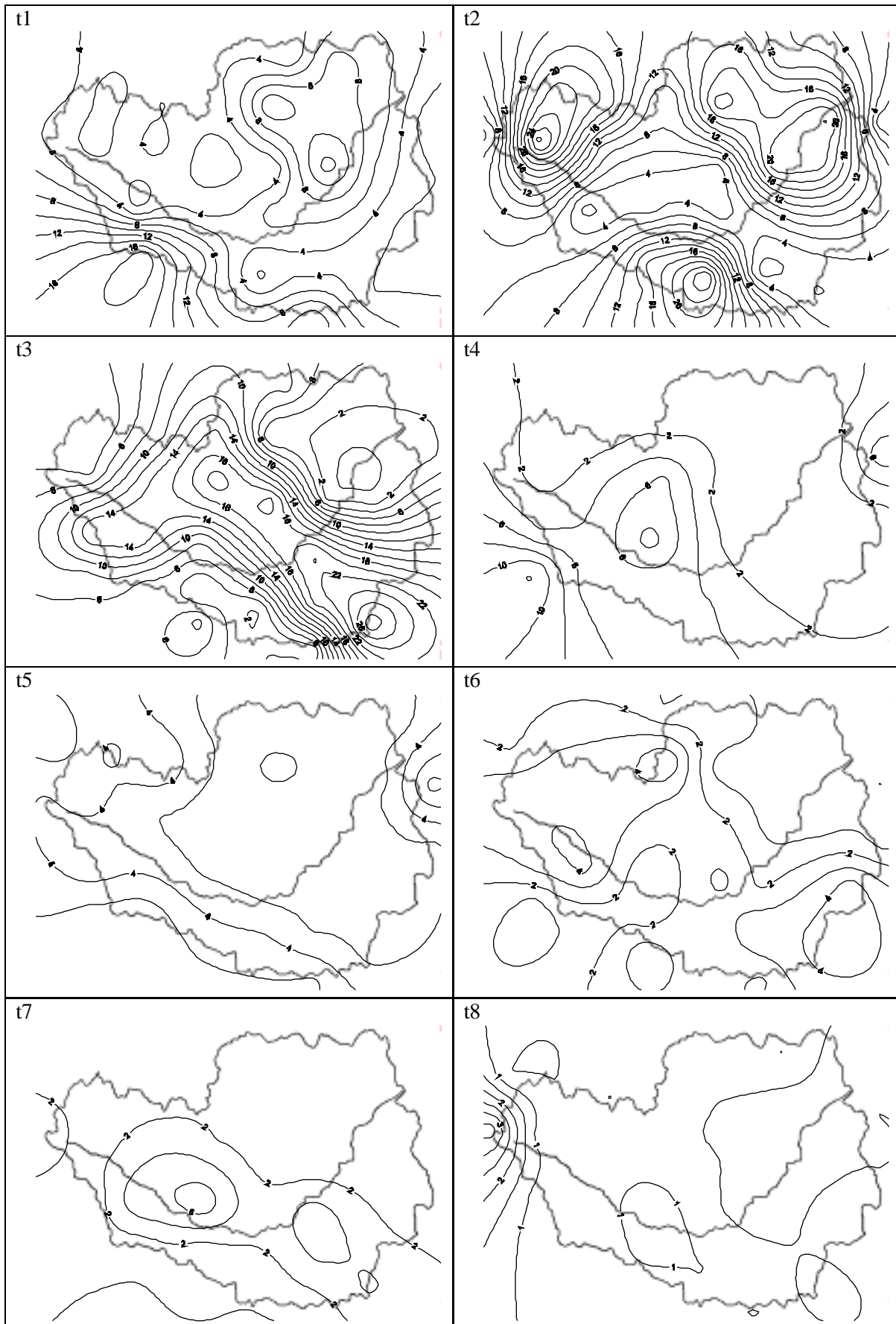Figure 5. Accumulated peak flow and excess runoff for the Category I storm.

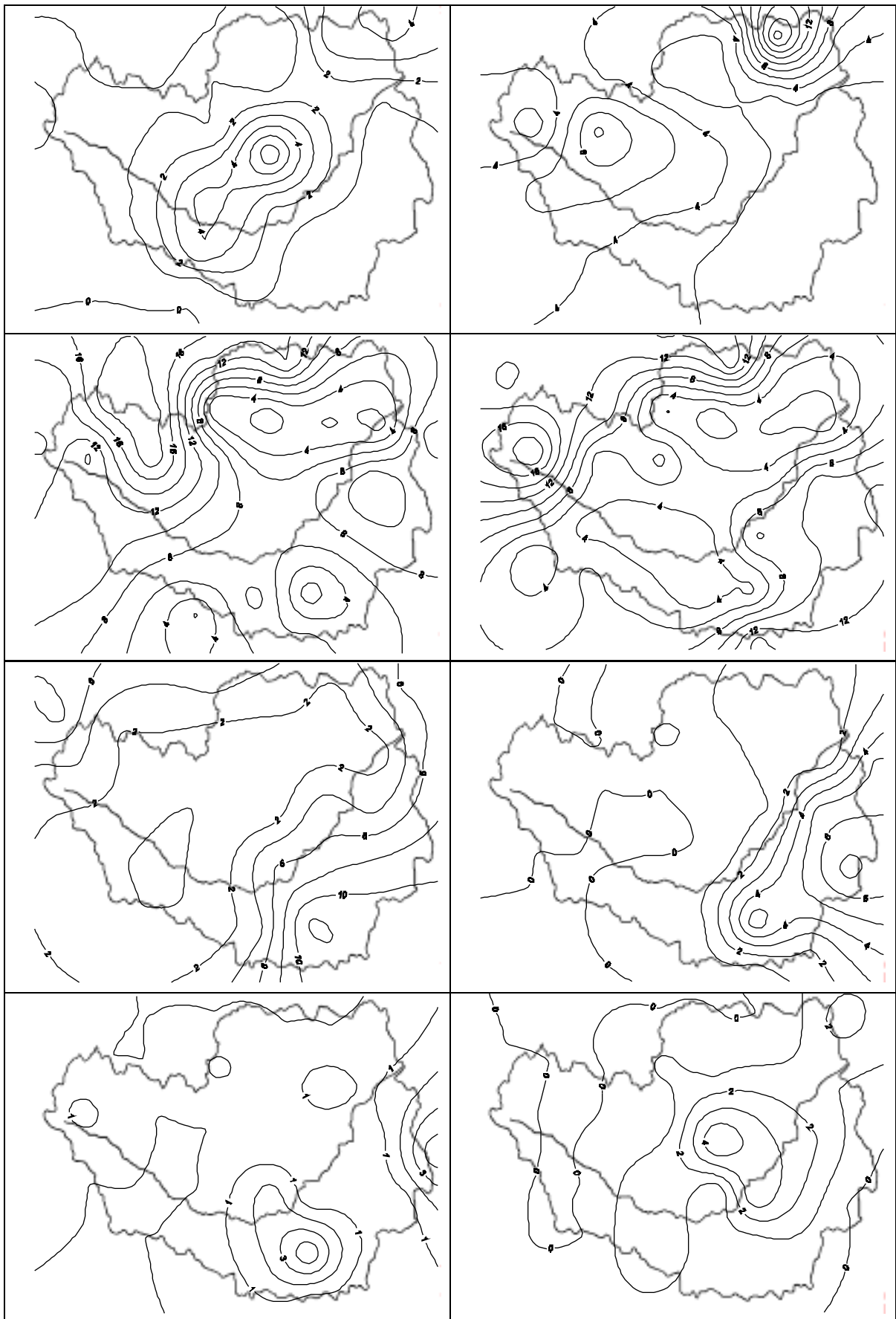Figure 6. August 18, 1964 storm 15-minute consecutive rainfall distribution pattern.

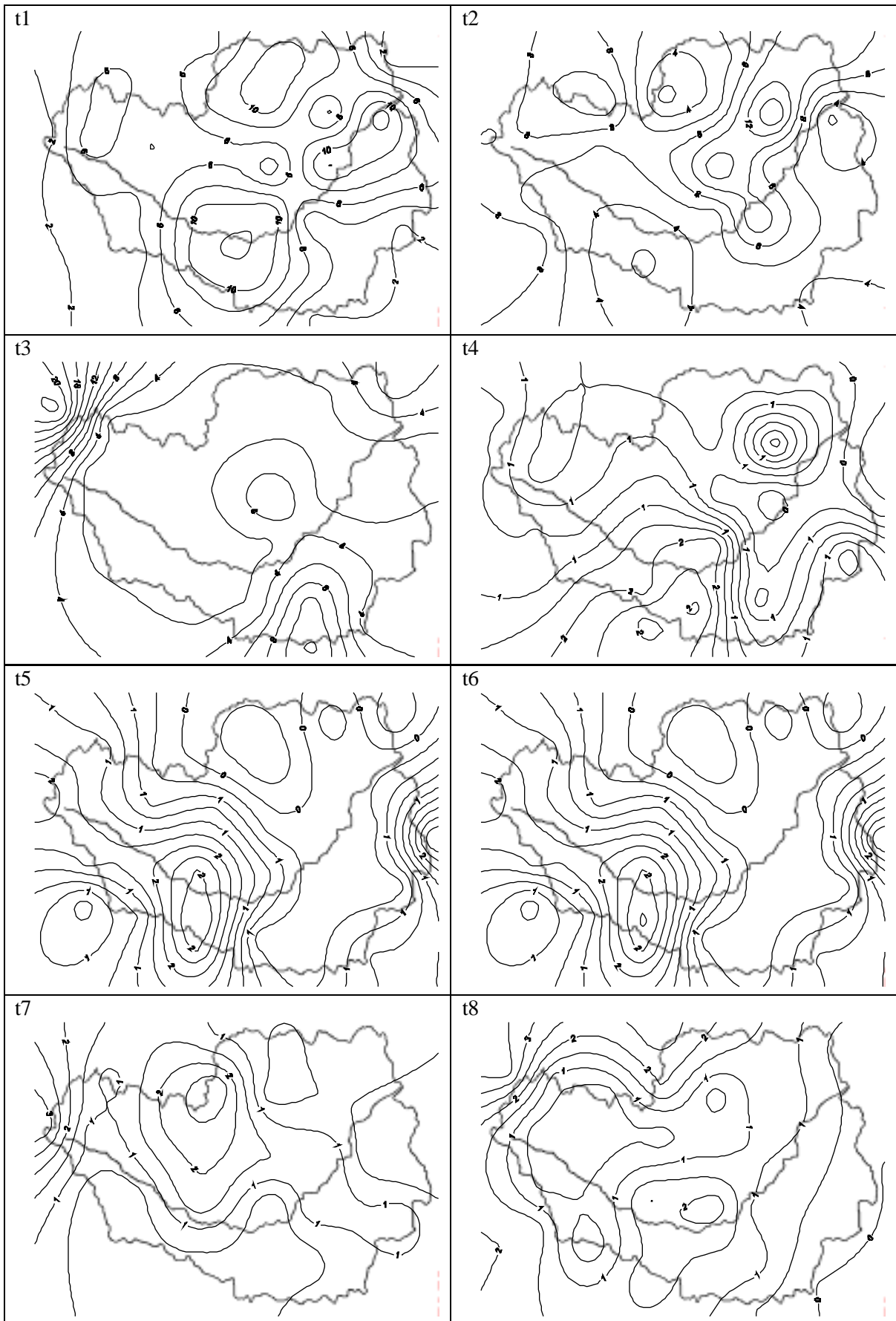Figure 7. November 16, 1964 storm 15-minute consecutive rainfall distribution pattern.

Figure 8. September 19, 1965 storm 15-minute consecutive rainfall distribution pattern.

In contrast, the cellular structure of the September 19, 1965 storm exhibited a somewhat different picture. Except for the first 45 minutes of the storm, the rain cells were low in intensity and covered limited areas of the basin. Moreover, they developed far from the outlet. Therefore, the time of maximum rainfall and its location caused a delayed effect on the Q_a in the downstream direction. Another group of cells begins to emerge during the second hour, but they are still low intensity. These cells, however, kept the flow relatively higher, but were not able to prevent the delay in the time of the peak flow. It is also important to note that these cells were not as persistent as those observed in the November 16, 1964 storm. When the cells are not persistent in time and move quickly, they will tend to produce lower flows compared to another storm which has exactly same rainfall intensity but moves slower. This also explains why the excess runoff from these storms displayed insignificant variability and its magnitude decreased gradually in a downstream direction. Another interesting feature of the September 19, 1965 storm is the presence of a sudden increase in peak flow near the basin outlet. It should be remembered that this storm has two different phases from a temporal perspective. After the first phase ends, another group of cells emerge over the basin within a few hours and cover a great portion of the basin. Increase in the peak flow is probably the result of this second phase of the storm, which was effective near the outlet. The excess runoff depth, however, did not significantly respond to this second phase of the storm. This is possibly due to the fact that the rain cells were low in intensity and had limited coverage.

Category II Storms

The next simulation included the May 9, 1965 and May 10, 1965 storms, both of which were characterized by low rainfall totals and short durations. While the May 9, 1965 storm is characterized by several areas where the rainfall intensity is high and the distribution is uneven, the May 10, 1965 storm exhibited a pattern characterized by low intensities and a relatively uniform spatial distribution (Figures 9 and 10). The rainfall distribution characteristics of these storms are reflected in their accumulated peak flows and runoff depths. The May 10, 1965 storm, characterized with low rainfall intensity and uniform spatial rainfall distribution, resulted in less variable and lower magnitude accumulated peak flow in the central and downstream parts (Figure 11). On the other hand, as seen in the example of the May 9, 1965 storm, the accumulated peak flow may exhibit more variability as a response to uneven distribution of high intensity rain cells. The May 9, 1965 storm had an uneven rainfall distribution with high intensity cells emerging within short time intervals at varying locations in the basin. In such cases, the rain producing cells fill depressions quickly and contribute to an increase in the streamflow. Once the precipitation losses were satisfied early in the storm, any rainfall excess easily became runoff, caused larger flows, and an early peak. Rainfall distribution characteristics of these two storms are also clearly reflected in their accumulated runoff depth in the downstream direction (Figure 11). Uneven distribution of precipitation and the presence of several high rainfall intensity areas with the May 9, 1965 storm cause substantial variability in R_a. In contrast, the May 10, 1965 storm produced accumulated runoff depths with less variability.

The final comparison focuses on storms of low total rainfall and long duration and includes the September 20, 1965 and May 10, 1964 storms. The graph of peak flow for the May 10, 1964 storm shows a steady rise in the upstream area, then levels off and takes another rise in the centroid of the basin (Figure 11). It remains nearly unchanged as it gets close to the basin outlet. The storm rainfall distribution indicates the presence of two high intensity cells which exactly match the location of the peak flow (Figure 12). A major portion of the storm precipitation is received in the central parts of the basin, which explains the initial variability observed with the Q_a in the upstream and central parts. Although the rainfall received in the early hours of the storm was able to produce an early increase
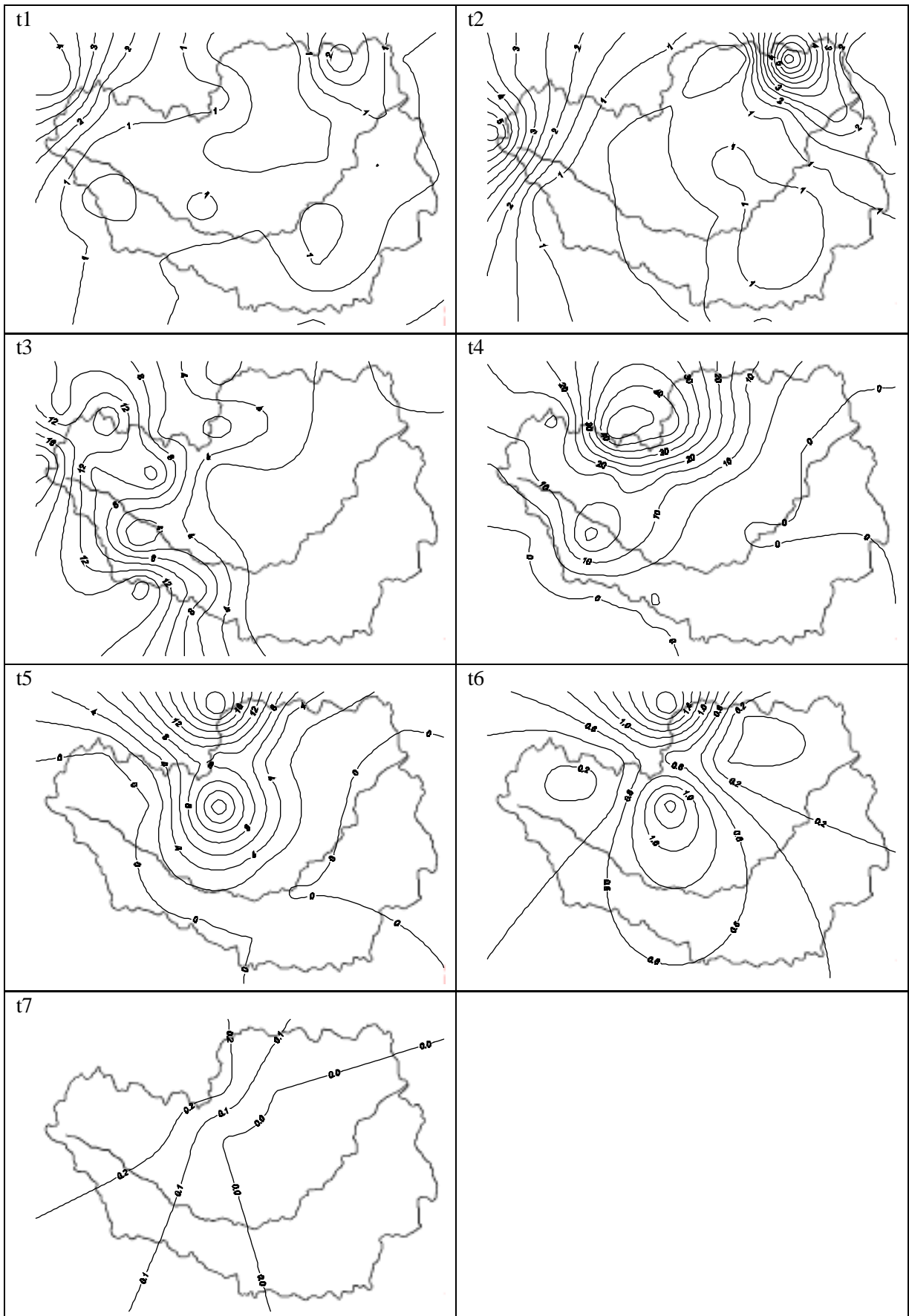
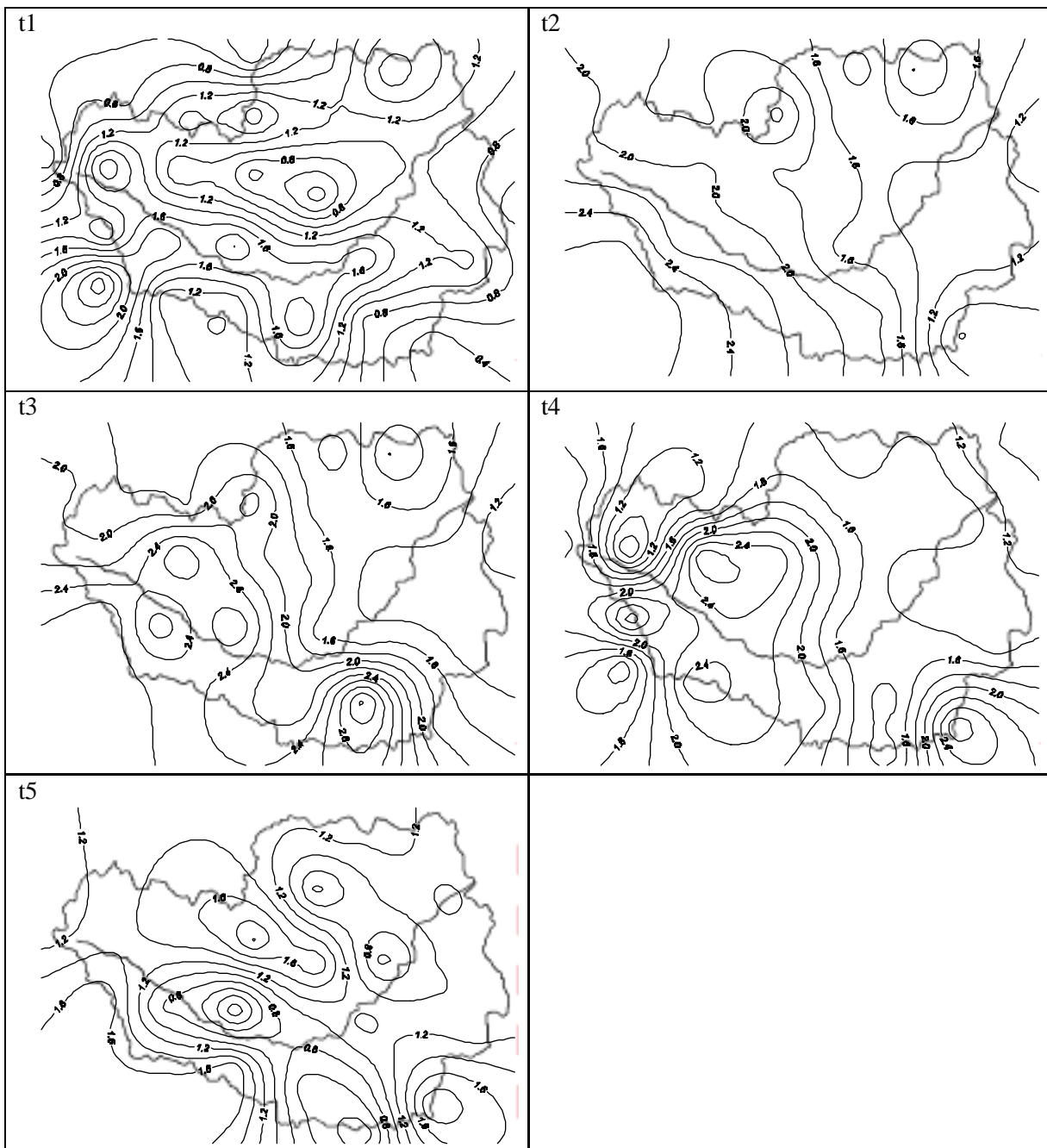Figure 9. May 9, 1965 storm 15-minute consecutive rainfall distribution pattern.

Figure 10. May 10, 1965 storm 15-minute consecutive rainfall distribution pattern.

in the peak flow due to its proximity to the outlet, the magnitude of the rainfall excess was not large enough to produce a high-accumulated peak flow.

One distinct feature of the September 20, 1965 storm is that several rain cells developed early in the event, increased in intensity, and moved slowly while growing in size (Figure 13). Moreover, the rain cells usually developed close to the basin outlet, which can easily trigger a high peak flow. But because only the upper and lower portions of the basin received significant amounts of rainfall, runoff contributions from the remaining parts of the basin to the accumulated Q_a were minor, and thus the accumulated peak flow did not exhibit significant variability. The storm pattern observed in the May 10, 1964 storm was different in the sense that the cell movement over the basin was rapid and exhibited an inconsistent spatial pattern. Furthermore, the intensities were usually low throughout the
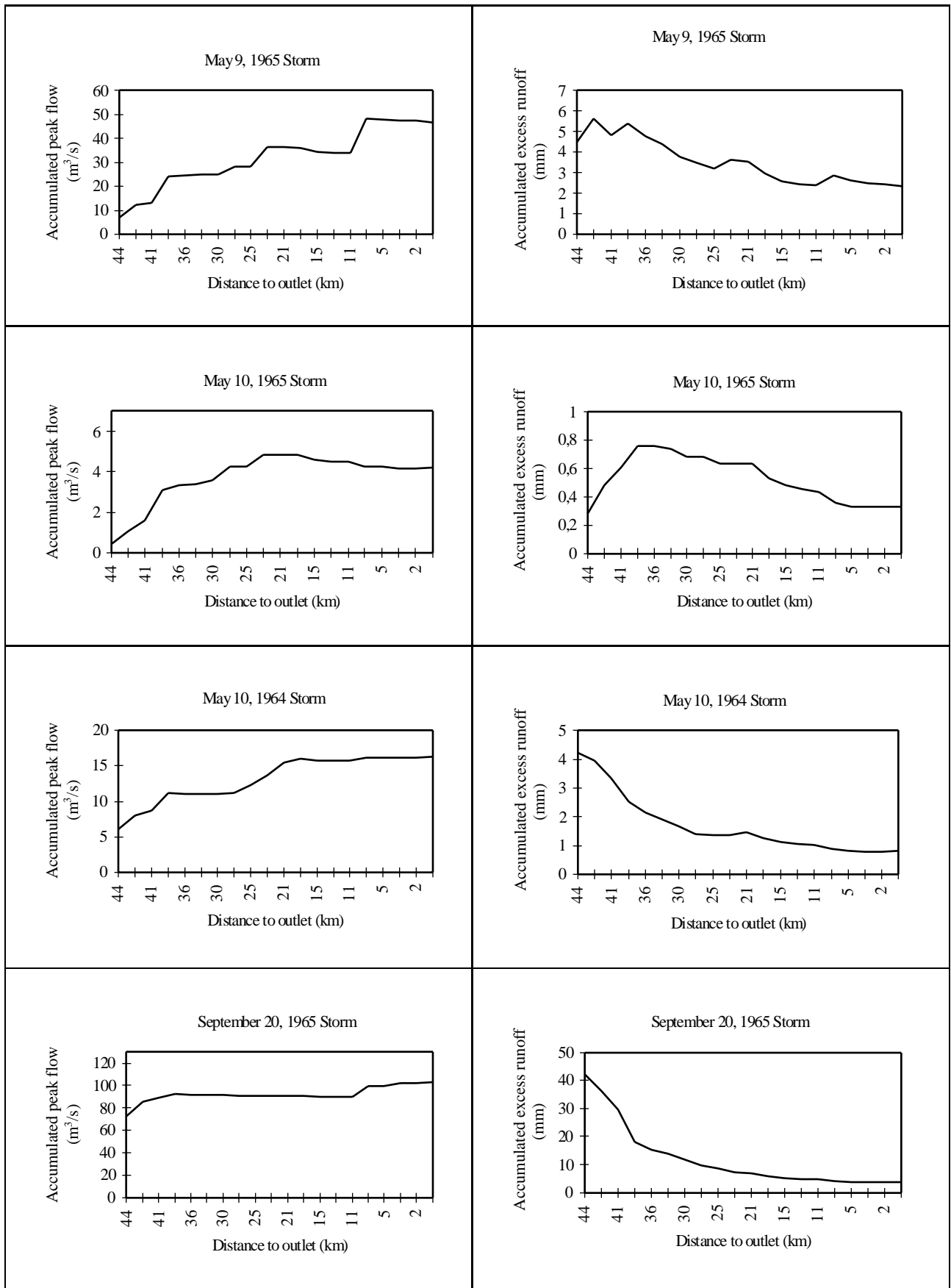
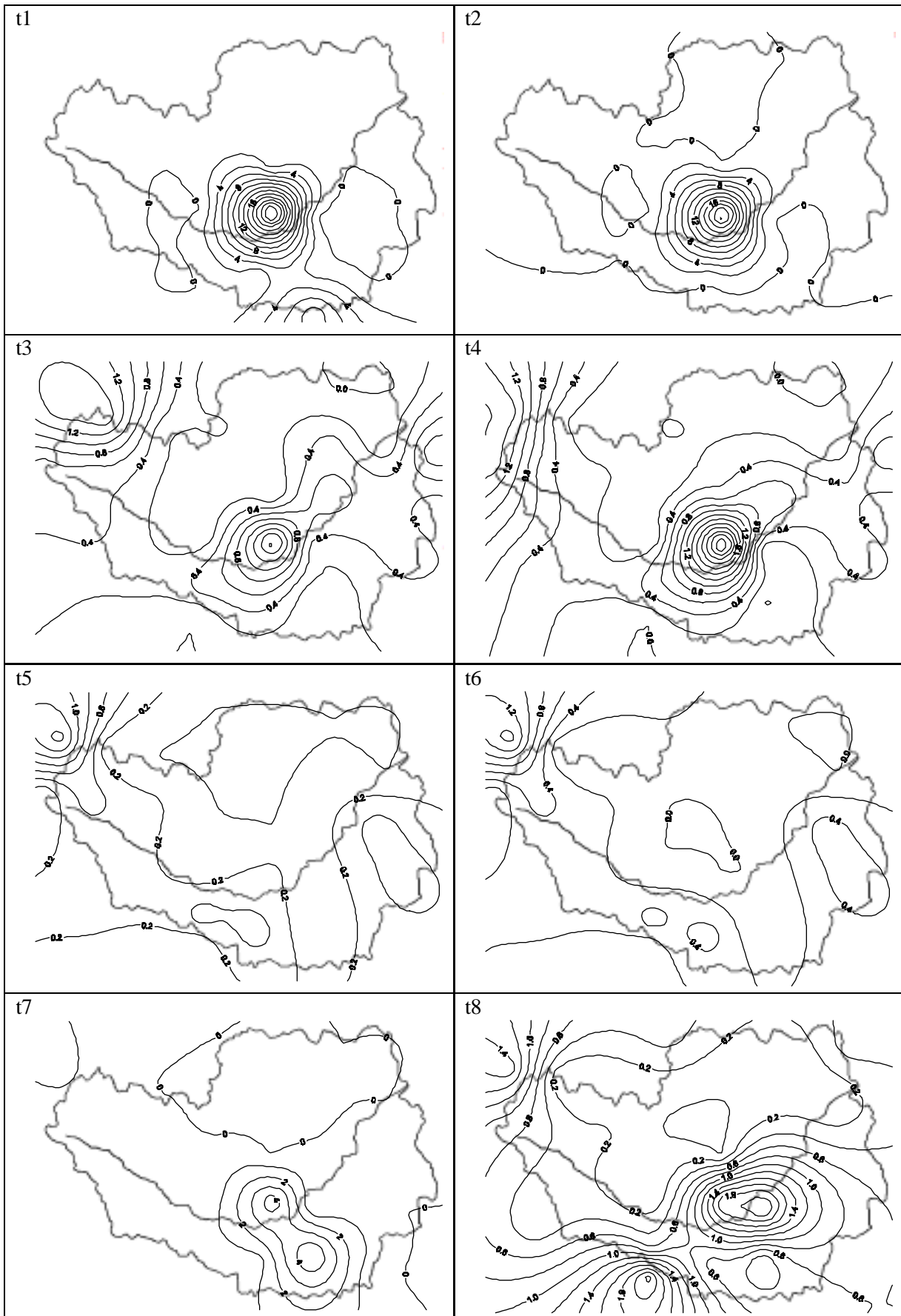Figure 11. Accumulated peak flow and excess runoff for the Category II storms.

Figure 12. May 10, 1964 storm 15-minute consecutive rainfall distribution pattern.
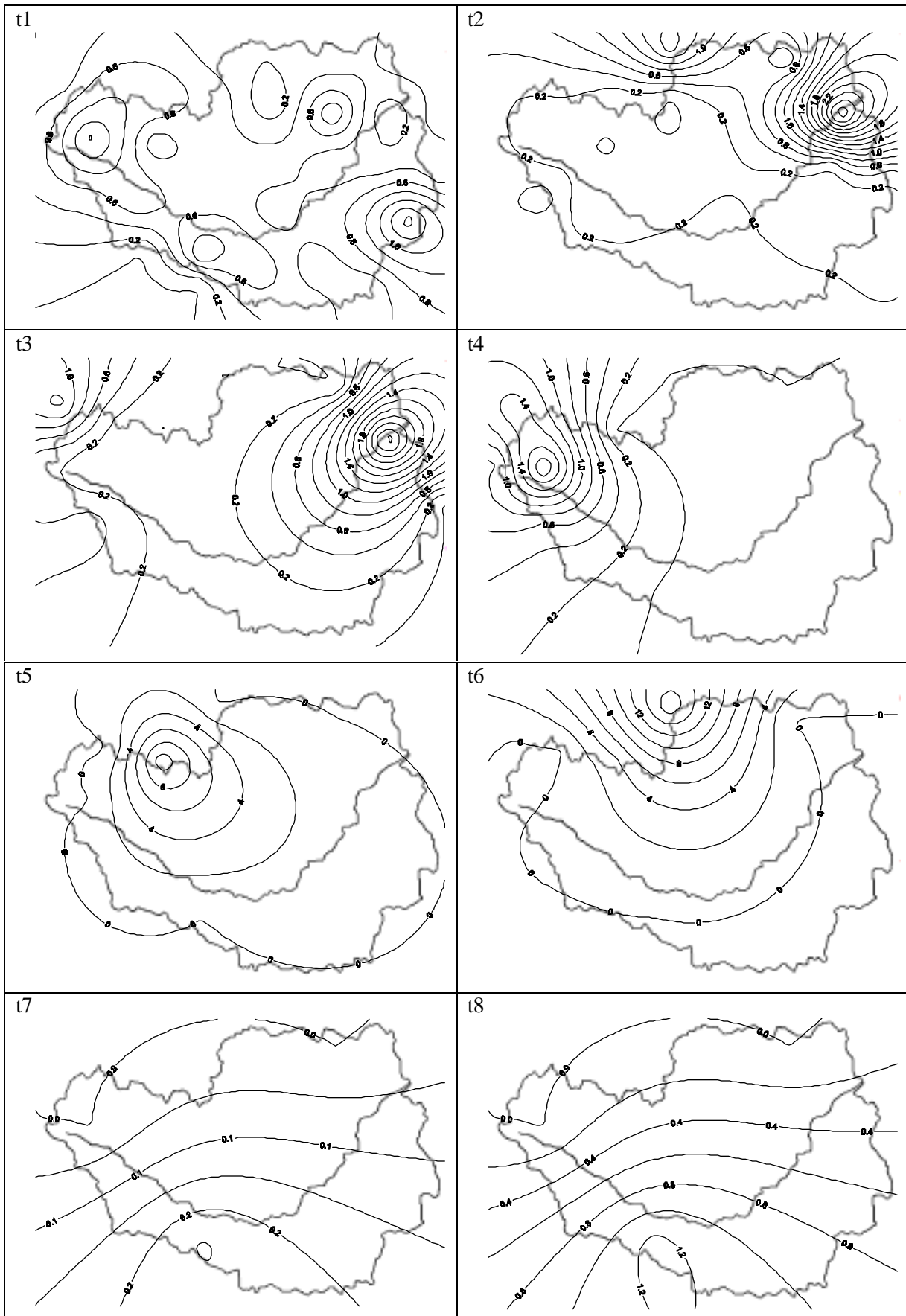
Figure 13. September 20, 1964 storm 15-minute consecutive rainfall distribution pattern.

storm, and the cell sizes were small. Throughout the storm, the high rainfall intensity areas quickly diminished. Such storm patterns usually result in low flow volumes and more variable peak flows. Low flow volumes with these storms also explain the small magnitude observed with the accumulated runoff depths in a downstream direction. Since the contribution from the new subwatersheds along the way will be insignificant, the magnitude of R_a varies slightly.

CONCLUSIONS

This study emphasizes the fact that accumulated peak flow and excess runoff can vary considerably in the downstream direction in response to variations in spatial and temporal distribution of rainfall. Some major conclusions from this study are:

1) The variability of Q_a and R_a depends not only on duration and magnitude of the rainfall but also largely on spatial distribution of rainfall and proximity of high intensity rain cells to the basin outlet. Larger variabilities are observed when rainfall is distributed non-uniformly and has high intensities. The resulting accumulated rainfall excess will be high in magnitude and will exhibit sudden peaks.

2) On the other hand, when the distribution of rainfall is more even, the resulting runoff is characterized by lower flow volumes and delayed peaks. The contributions from the new subwatersheds to the accumulated peak flow in a downstream direction are usually less if the high intensity rainfall areas are located far from the centroid of the basin. Coupled with the steady increase in drainage area in the downstream direction, changes in the magnitude and variability of Q_a will remain relatively low. This also explains why the accumulated runoff depth does not vary substantially in the downstream direction even though the rainfall distribution may be nonuniform. Thus, the storms which concentrate over the basin in a nonuniform manner, may still cause greater variability in the accumulated runoff depth than a uniform storm having the same magnitude.

3) Variability of the accumulated peak flow rates is more pronounced as rainfall depth increases. With increasing basin average precipitation, chances of accurately simulating the hydrograph components increase as well. For high storm totals, flow volumes and peak flow can be simulated more accurately as compared to the hydrographs obtained from the low storm totals. Thus, the importance of temporal and spatial scales may be less for higher rainfall storms in predicting peak flows and flow volumes. The temporal distribution of rainfall can considerably influence the time and rate of peak flow. It has been observed that if the storm peaks early and if the distribution of rainfall is uniform, the peak runoff is less than for a storm having the same average intensity.

Thus, the usual spatial and temporal representations of basin precipitation obtained, for example, from gage densities of less than one gage per 4000 km^2 and recorded at hourly intervals (commonly available form National Weather Service networks) may be inadequate to accurately resolve runoff hydrographs from basins of approximately 500 km^2, particularly during periods of low rainfall intensity. More precise measurements of precipitation and antecedent moisture conditions will probably reduce the input errors reflected in simulation results.

FINAL REMARKS

It is expected that surface runoff characteristics will have certain impacts on soil and water conservation treatments applied in the watershed. Identifying the potential impacts, which the varying runoff conditions might have on soil and water conservation treatments, requires further research. In particular, soil conservation practices such as terraces, diversions and floodwater-retarding reservoirs might be affected by changing spatial patterns in surface flow. New procedures

for estimating erosion and sediment yield in the watershed may be developed in the light of variations in runoff across the watershed. This study may further lead to a reassessment of the present applications in the basin in terms of designing more efficient soil and water conservation practices that fit the surface runoff conditions of the basin presented in this study. In particular, the effect of the SCS flood-control program on downstream flow regime of the Little Washita River can be reevaluated for stormy weather conditions.

ACKNOWLEDGMENTS

REFERENCES

Allen, P.B., and J.W. Naney; Hydrology of the Little Washita River Watershed, Oklahoma: Data and Analysis. U.S.D.A. Research Service, Water Quality and Watershed Research Lab, Durant, OK, 74pp, 1991.

Beven, K.J., and G.M. Hornberger; Assessing the effect of spatial pattern of precipitation in modeling streamflow hydrographs. Water Resources Bulletin, 18, 823-829, 1982.

Duchon, C. C., J.M. Salisbury, T.H.L. Williams, and A.D. Nicks; Application of satellite remote sensing to basin hydrology. Water Resources Research, 28, 527-538, 1990

Duchon, C.E., and J.M. Salisbury, T.H. Williams, and A.D. Nicks; An example of using Landsat and GOES data in a water budget model. Water Resources Research, 28, 527-538, 1992

Garbrecht, J.; Effects of Spatial Accumulation of Runoff on Watershed Response. Journal of Environmental Quality, 20,31-35, 1991.

Goodrich, D.C. and D.A. Woolhiser; Catchment Hydrology, U.S. National Report to International Union of Geodesy and Geophysics, 1987-1990. American Geophysical Union, 1990

Hoggan, D.H.; Computer Assisted Flood Plain Hydrology and Hydraulics, McGraw Hill, New York, 1989.

Hromadka, T.V. II.; Use of sub-basins in rainfall- runoff models, I: Development of a multi-linear runoff model approximation. Hydrological Science and Technology, 3 (1-2), 25-35, 1987a.

Hromadka, T.V. II.; Use of sub-basins in rainfall-runoff models, II: Reducing model uncertainty. Hydrological Science and Technology, 3 (1-2), 37-45, 1987b.

Komuscu, A.U.; Impact of the Spatial and Temporal Variability of Precipitation on Simulating Runoff Hydrographs, Ph.D. Dissertation, University of Oklahoma. Norman, OK, 1993.

Legates, D.R., and A.U. Komuscu; Impact of the Spatial and Temporal Variability of Precipitation on Simulating Runoff Hydrographs, 1997 (submitted to Journal of the American Water Resources Association).

Linsley, R.K., and W.C. Ackerman; Method of Predicting Runoff from Rainfall, Paper 2147, American Society of Civil Engineers, New York, 1942.

McCuen, R.H.; A Guide to Hydrologic Analysis Using SCS Methods. Prentice Hall, Inc. Englewood Cliffs, New Jersey, 1982.

Nicks, A.D.; Modeling off-site impacts. Proceedings of the Symposium, Committee on Basin Management, Irrigation and Drainage, American Society of Civil Engineers, April 30-May 1, Denver, CO, 1985.

Nicks, A.D.; Off-site sediment impacts using basin scale simulation. Proceedings of the Fourth Federal Interagency Sedimentation Conference, Vol.2, 6-137 to 6-147, 1986.

Niemczynowicz, J.; The rainfall movement - A valuable complement to short-term rainfall data. Journal of Hydrology, 104, 311-326, 1986.

Osborn, H.B.; Storm-Cell Properties Influencing Runoff From Small Watersheds. Transportation research Board.

National Research Council. National Academy of Sciences, Washington D.C., Transportation Research Record, 922, 24-32, 1984.

Raudkivi, A.J.; Hydrology: An Advanced Introduction to Hydrologic Process and Modelling. Pergamon Press. Oxford, Great Britain, 479 pp, 1979

 Salisbury, J.M.; Basin Controls and Hydrologic Response in the Little Washita River Basin,   Oklahoma. Ph.D. Thesis. University of Oklahoma, Norman, OK, 1992.

Silverman, B.A., L.K. Rogers, and D. Dahl; On the sampling variance of raingage networks. Journal of Applied Meteorology, 20, 1468-1478, 1981.

Soil Conservation Service ; National Engineering Handbook, Section 4: Hydrology, U.S. Department of Agriculture, Washington D.C., 1964.

Staff, Water Quality and Watershed Research Laboratory. Hydrology, Erosion, and Water Quality Studies in the Southern Great Plains Research Watershed, Southwestern Oklahoma, 1961-78, United States Agricultural Research Service Report ARM-S29, 175pp, 1983.

Stephenson, D., and M.E. Meadows; Kinematic Hydrology and Modelling, Developments in Water Science, 26, Elsevier Publishing Comp., New York, 1986.

U.S. Army Corps of Engineers; HEC-1 Flood Hydrograph Package. User's manual: Version 4.0, Davis, CA., 283pp, 1990.

ADDRESS FOR CORRESPONDENCE

Dr. Ali Umaran Komuscu
State Metereological Service
Research Department
Kalaba, Ankara 06120
TURKEY

E-mail: aukomuscu@meteor.gov.tr